Elastic Scattering and Single Meson Production in Proton-Proton Collisions at 2.85 Bev*

G. A. SMITH,†‡ H. COURANT, E. C. FOWLER, H. KRAYBILL, J. SANDWEISS, AND H. TAFT
Physics Department, Yale University, New Haven, Connecticut, and Brookhaven National Laboratory, Upton, New York

(Received April 19, 1961)

The Brookhaven National Laboratory twenty-inch liquid hydrogen bubble chamber was exposed to a monoenergetic beam of 2.85-Bev protons, elastically scattered from a carbon target in the internal beam of the Cosmotron. All two-prong events, excluding strange particle events, have been studied by the Yale High-Energy Group. The remaining interactions have been studied by the Brookhaven Bubble Chamber Group. Elastic scattering was found to be mostly pure diffraction scattering at center-of-mass angles up to about thirty-five degrees. Some phase shift and/or tapering of the proton edge was required to fit the data at larger angles. No polarization effects in the proton-carbon scattering were observed using hydrogen as an analyzer of polarized protons. Nucleonic isobar formation in the $T=3/2$, $J=3/2$ state was found to account for a large part of single pion production. High- orbital angular-momentum states were found to be greatly favored in single pion production. The isobar model of Lindenbaum and Sternheimer gave good agreement with the observed nucleon and pion energy spectra. No polarization or alignment effects were observed for the isobar assumed in this model.

I. INTRODUCTION

A NUMBER of workers,[1–5] employing either the cloud chamber, electronic counters, or nuclear emulsion as a detecting device, have investigated proton-proton interactions in the 2–3 Bev kinetic energy region, however no detailed or statistically significant experiment had been done on the general problem of proton-proton interactions, particularly the inelastic interactions, in this energy range as of late 1959. To investigate this energy region more completely, the Brookhaven National Laboratory twenty-inch liquid hydrogen bubble chamber[6] was exposed to a beam of 2.85-Bev protons, elastically scattered from a carbon target in the internal beam of the Cosmotron.

At these energies, proton-proton elastic scattering has been described from previous counter and emulsion experiments.[2,5] Since the initial elastic scatter of the Cosmotron internal beam was believed to be inside the first diffraction scattering minimum of carbon, it was of some interest to look for a right-left asymmetry in the proton-proton elastic scatter in the chamber. Also, considering the small number of single meson production events which the Brookhaven Cloud Chamber Group had found at 2.75 Bev,[1] it was estimated that the analysis of approximately 1500 two-prong inelastic events would be sufficient to significantly improve the momentum and angular distributions of $pn\pi^+$, $pp\pi^0$, and $d\pi^+$. Various models have been proposed to account for pion production in nucleon-nucleon collisions. Of particular interest in this experiment was the possible influence of a nucleonic isobar state of isotopic spin $T=\frac{3}{2}$, total angular momentum $J=\frac{3}{2}$, on the pion production. Since the pion-nucleon interaction in this state is well known, it was felt that the demonstration of its existence in the proton-proton interaction would be an aid to the analysis of the general problem of nucleon-nucleon interactions at these energies.

II. PROTON BEAM

Figure 1 shows the general proton beam setup of this experiment at the Cosmotron. When the internal proton beam reached the desired energy of approximately 3 Bev, the rf-accelerating field was turned off and the rapid-beam ejector was fired. This device[7] includes a pair of parallel rectangular coils of size one foot by five feet, separated by a nine-inch gap which is pulsed so as to induce strong betatron oscillations in a large fraction of the internal beam. It is believed that at the time of this experiment the n value of the Cosmotron was approximately 0.6. As a result of the betatron oscilla-

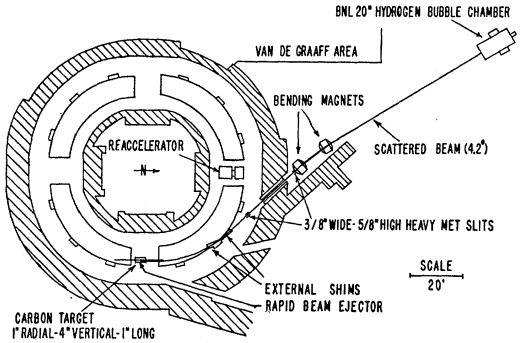

FIG. 1. Scattered 2.85-Bev proton beam at the Cosmotron.

* Supported in part by the U. S. Atomic Energy Commission.
† Based on work submitted to the faculty of the Graduate School of Yale University by G. A. Smith in partial fulfillment of the requirements for the degree of Doctor of Philosophy.
‡ Supported by the Socony Mobil Oil Fellowship in Physics, 1960–61.
[1] W. B. Fowler, R. P. Shutt, A. M. Thorndike, W. L. Whittemore, V. T. Cocconi, E. Hart, M. M. Block, and E. M. Harth, Phys. Rev. **103**, 1484 (1956).
[2] B. Cork, W. A. Wenzel, and C. W. Causey, Jr., Phys. Rev. **107**, 859 (1957).
[3] F. F. Chen, C. P. Leavitt, and A. M. Shapiro, Phys. Rev. **103**, 211 (1956).
[4] M. J. Longo, J. A. Helland, W. N. Hess, B. J. Moyer, and V. Perez-Mendez, Phys. Rev. Letters **3**, 568 (1959).
[5] W. M. Preston, R. Wilson, and J. C. Street, Phys. Rev. **118**, 579 (1960).
[6] D. C. Rahm, *Proceedings of the International Conference on High-Energy Accelerators and Instruments* (European Organization for Nuclear Research, Geneva, 1959), p. 440.
[7] D. C. Rahm, Bull. Am. Phys. Soc. **2**, 11 (1957); a final report on this device has been submitted to Rev. Sci. Instr.

tions the beam was driven into a target somewhat inside the rapid beam injector. A 1 in. radial, 4 in. vertical, 1 in. long carbon target was placed about 2 in. radially inward from the rapid beam ejector coils in the east straight section. The internal beam of about one square inch cross section was driven in radially by the rapid-beam ejector over a period of a few microseconds.

The ultimate goal of this beam design was a well-collimated, monoenergetic beam of protons with sufficient intensity and pulse-to-pulse stability. Elastically scattered protons from the carbon target at $4.2°\pm0.3°$ relative to the beam direction in the straight section had a momentum appropriate for continuing through the remaining part of the straight section, part of the Cosmotron quadrant, and out through a thin window in one of the pumping stations in the vacuum system. The size of the carbon target was adjusted to give the desired number of protons in the beam. A set of iron shims was placed inside and outside the pumping station exit to keep the beam focused in the fringing field and also to help direct the beam through a portal in the main shielding. After leaving the quadrant through the external shims, the beam passed through a Hevimet slit and then an iron collimator in the main shielding. Outside the main shielding another Hevimet slit was used to help restrict the beam to those rays which would traverse the bubble chamber thin window. Two bending magnets at 15 kgauss were then used to sweep out low momentum products of slit scattering and to rid the beam of neutrals. The beam was adjusted to pass through the central region of the Brookhaven twenty-inch chamber approximately 100 feet from the sweeping magnets.

Calculations of the trajectories of the beam were carried out at Brookhaven using the known values of the Cosmotron magnetic field.[8] The beam was elastically scattered to within $\pm1\%$ in momentum according to these calculations. The total bending of the beam in the Cosmotron field was about 40° and the main momentum analysis of the beam occurred in this bending.

III. SCANNING AND MEASURING

Overall, approximately 90 000 photographs were taken of 2.85-Bev proton-proton interactions in the chamber. Approximately 9000 photographs were scanned in order to obtain 25000 two-prong events. An independent rescan was made of all 9000 photographs. All scanning was done on one of the two Yale scanning machines. Any three of the four 35-mm films from the twenty-inch chamber, with the appropriate arrangement of lenses and two large mirrors, could be projected onto a horizontal table at about life size. Continuously-variable-speed motors on the film advance mechanism, allowed the scanner to move any number of films in either direction. A combination of mechanical and vacuum clamping of the film was used, resulting in a very sharply focused image on the table. Scanners were instructed to look for all two-prong interactions in a reduced area in the chamber. A rough check of the azimuth angle of each event beam track was made to eliminate any stray track events. Beam counting was done for cross-section purposes. The combined efficiency for any two independent scans was found to be 98%. This figure is exclusive of loss in small angle elastic scattering which will be discussed later.

All measurements were done on the Yale manually operated measuring engine. The films are mounted on a precision stage and are projected onto a screen in front of the measurer at about three times lifesize. The measurer employs a rotatable cross hair in the center of the screen to set on a track. Rotary encoders are connected directly to the stage lead screws and put out x and y coordinates for each measurement. Pulses from the encoders are converted into decimal numbers and punched out on standard eight-word IBM cards. A complete measurement consisted of seven punched cards. The first card contained an identifying event number, fiducial measurements, magnet current information, and an event type to be interpreted by a computer. This was followed by two cards for each of the three tracks (beam and two secondaries). Each track was measured in the optimum pair of stereoscopic views of the four films.

IV. EVENT ANALYSIS

All events whose two prongs were split by the direction of the incoming beam and which could therefore be elastic scatterings, were processed by a system set up for the Yale IBM 650 computer. A plot of the measured beam momenta for these events with beam tracks longer than 20 cm, gave p (average) $=3670$ Mev/$c\pm1\%$ with a full width at half maximum of $\pm3\%$. For each event processed, a coplanarity volume F was computed, where

$$F=(\mathbf{N}_1\times\mathbf{N}_2)\cdot\mathbf{N}_3, \tag{1}$$

and $\mathbf{N}_1$, $\mathbf{N}_2$, and $\mathbf{N}_3$ are unit vectors in the directions of the three tracks. F is zero for a coplanar event and has a maximum value of one. A plot of F showed a sharp peaking around zero and negligible background inside the limits -0.01 to 0.01. The space angles θ_2 vs θ_3 were also plotted and a quantity θ_1, defined as the perpendicular distance from each event to the theoretical curve for p-p elastic scattering at 2.85 Bev, was determined. A plot of θ_1 showed a sharp peaking at 0° and negligible background outside of 1°. These limits, together with an upper limit on the missing mass of 120 Mev, were chosen to define elastic events. It was found on the basis of a later and more complete treatment, that elastics could be well separated from inelastics by just these

[8] J. Sandweiss, Brookhaven National Laboratory internal report, 1959 (unpublished). The authors wish to thank Dr. R. M. Sternheimer for supplying correct values of the Cosmotron magnetic field.

criteria. Although most of the elastic events passed only these tests, a small additional sample was added from the later treatment of inelastics on the IBM 704.

In order to achieve uniform, systematic processing of a large number of events, a system was set up for the IBM 704 computer under the code name YACK, which is sufficiently general to handle many different types of events. This system is divided into two parts, reconstruction and kinematic fitting, which are essentially separate and independent, although each event is processed completely in a single pass in order to simplify the later analysis.

The reconstruction phase of the system proceeds first by scaling and orienting the input data to coordinate systems fixed in the chamber, using known fiducial positions on the front glass. Since corresponding points are not measured, each point in one of an arbitrary pair of views is mapped onto a circle through the three neighboring points in the second view and from this mapping, the true three dimensional point is easily constructed. This calculation is accomplished by an iterative method which is essentially exact except for the circular interpolation. Once the points in space corresponding to a given track are known, a least-squares fit to a helical spiral is made, which takes into account the non-linear loss of momentum of a particle as it traverses the material of the bubble chamber, as well as the variation of the magnetic field over the chamber volume.[9]

An important feature of this phase is the error calculation. Errors on the azimuthal angle, dip angle, and projected curvature of each track, as well as the correlation between these quantities are computed from the least-squares error matrices for the fit.[10] In addition, multiple-scattering errors are included in the form derived by Willis.[11] The result is a three-by-three error matrix for each track computed both at the beginning and at the end of the track. This error matrix is then used, together with the measured variables of the track, as the input to the kinematic phase of the program. The reconstruction phase has been written in such a way that up to nine tracks with six mass assignments per track may be easily accommodated.

The kinematic fitting phase of the system is based on the use of a subroutine with the code name GUTS.[12] This routine constructs a χ^2 function,

$$\chi^2=\sum_{i,j}(x_i-x_i^m)G_{ij}(x_j-x_j^m), \qquad (2)$$

where x_i^m are the measured variables and the G_{ij} are the inverse error matrices. This function is then minimized subject to the constraints of energy and momentum balance, and the set of variables x_i thus obtained are used in all future analysis. Since the minimizing procedure is quite general and is applicable to many different classes of interaction vertices, a general routine has been set up to fit every reasonable set of hypotheses in any given experiment. In the present experiment each event was fit to the following six interpretations:

$$\begin{aligned} &p+p\rightarrow p+p, && p+p\rightarrow p+\pi^++n,\\ &p+p\rightarrow p+p+\pi^0, && p+p\rightarrow d+\pi^+, \qquad (3)\\ &p+p\rightarrow \pi^++p+n, && p+p\rightarrow \pi^++d. \end{aligned}$$

In order to reduce the total processing time, the program computed the missing mass and its error, based on the interpretation, which was about to be tried. If this mass was more than five standard deviations away from that required by the interpretation, the program skipped to the next interpretation.

Since an accurate knowledge of the errors was essential in this type of analysis, a careful determination of the mean measurement error propagated into the chamber was made. Denoting this error by ϵ, a consideration of the least-squares fitting procedure for the high-momentum beam tracks under the conditions of this experiment shows that the measured momentum should deviate from the average according to the formula

$$|p(\mathrm{Mev}/c)-3670|=2341\epsilon(\mathrm{microns})/L^2(\mathrm{cm}). \qquad (4)$$

A plot of this quantity for beam tracks of various lengths gave a value for ϵ of 35 μ. The entire error

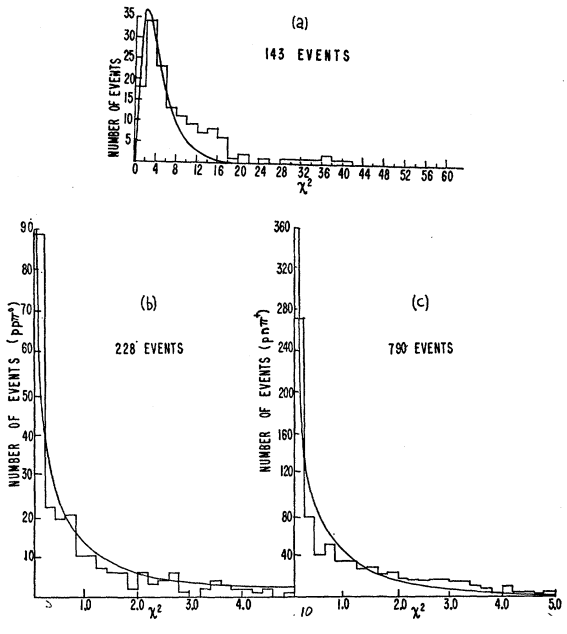

FIG. 2. (a) Experimental elastic scatter χ^2 distribution with the best fit theoretical curve for χ^2 less than eight. (b) Experimental $pp\pi^0$ χ^2 distribution with theoretical curve normalized to the area in the histogram. (c) Experimental $pn\pi^+$ χ^2 distribution with theoretical curve normalized to the area in the histogram.

[9] H. D. Taft, *Proceedings of the 1960 International Conference on Instrumentation for High Energy Physics* (to be published).
[10] G. A. Smith, Ph.D. thesis, Yale University (unpublished).
[11] W. Willis, Brookhaven National Laboratory internal report, 1959 (unpublished).
[12] J. P. Berge, F. T. Solmitz, and H. D. Taft, University of California Radiation Laboratory Report, 1960 (unpublished).

matrix was then constructed using this figure together with known multiple scattering errors. Each inelastic event with a χ^2 less than five was examined by a physicist and an interpretation was made on the basis of the χ^2 value and ionization. Events for which the ionization was inconsistent with the fit, or which had no χ^2 less than five, were remeasured to ensure that no interpretation in terms of elastic scattering or single meson production was possible. The results of these remeasurements indicated that 7% of all events were poorly measured. The identification of elastic events was sufficiently clear-cut that no upper limit on χ^2 was required. The experimental χ^2 distributions are shown in Fig. 2.

V. ELASTIC SCATTERING

In this experiment a total of 1038 elastic scattering events were identified by analysis on the IBM 650 and 704 computers.[13,14] The center-of-mass angular distribution showed a strong peaking near 0°. Thus it was suspected that some events were missed by the scanner because of short recoil protons which might not have been seen in the chamber. Azimuthal distributions indicated that such an effect took place at laboratory scattering angles less than 2.5°. Since the distribution showed strong diffraction-type scattering near 0°, it was felt that all scattering at less than 2.5° would be most accurately accounted for by an optical model correction. Based on the number of events in a reduced fiducial volume, the cross section for elastic scattering at laboratory angles greater than 2.5° was found to be 12.87±0.69 mb.

The representation of a nucleus by a complex potential or index of refraction has been generally referred to as the optical model. The concept of the optical model discussed here was originally developed by Fernbach *et al.*[15,16] to account for the scattering of high-energy neutrons by nuclei. Because of the reasonable agreement of optical model calculations made by Cork *et al.*[2] with elastic scattering distributions at 2.24, 4.40, and 6.15 Bev, a similar treatment was made here. It has been demonstrated[16] that, for a large number of angular momentum states and small scattering angles, the scattering amplitude takes the form

$$f(\theta)=ik\int_0^R (1-ae^{i\delta})J_0(k\rho\sin\theta)\rho d\rho, \qquad (5)$$

where a is the amplitude of the transmitted wave for an incident wave of unit amplitude, δ is the phase of the transmitted wave for an incident wave of zero phase, the volume of interaction is a disk of radius R, ρ is the variable impact parameter, θ is the scattering angle, and k is the incident nucleon wave number. Three forms (models A, B, and C) have been considered here.

1. Model A—Purely absorbing disk with radius R. In this case the complex index of refraction is completely imaginary; thus $\delta=0$. Given the total elastic and absorption cross sections from the experiment, one may calculate a for any value of R since

$$\sigma_a=2\pi\int_0^R (1-a^2)\rho d\rho,$$
$$\sigma_e=2\pi\int_0^R |1-ae^{i\delta}|^2\rho d\rho. \qquad (6)$$

2. Model B—Absorbing disk with short-range phase shift. In this case set δ=constant for $0<\rho<R_1$, $\delta=0$ for $\rho>R_1$; a=constant for $0<\rho<R_2$, $a=0$ for $\rho>R_2$; and $R_1<R_2$. From Eq. (6), a and δ may be calculated, and the scattering amplitude follows from Eq. (5).

3. Model C—Tapered absorbing disk with short-range phase shift. In this case set δ=constant for $0<\rho<R_1$, $\delta=0$ for $\rho>R_1$; $1-a=A(1-\rho^2/R_2^2)$, with A=constant for $0<\rho<R_2$, $A=0$ for $\rho>R_2$; and $R_1<R_2$. From Eq. (6), A and δ may be calculated and the scattering amplitude follows from Eq. (5).

The experimental distribution with the optical model curves is shown in Fig. 3. The parameters listed are those which gave the best fit to the data. From model A the cross section for all elastic scattering at less than 2.5° in the laboratory was determined to be 2.45±0.31 mb. Thus, the total elastic cross section was 15.32±0.76

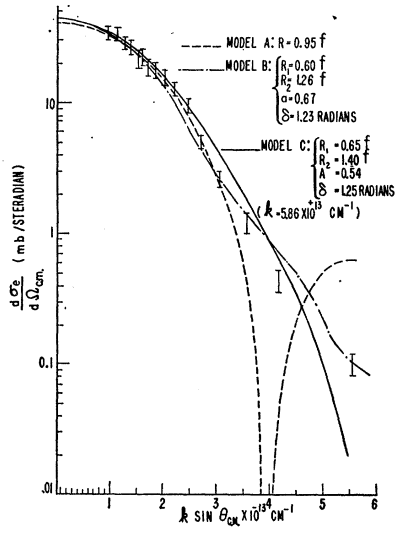

FIG. 3. Elastic scattering c.m. angular distribution with optical model curves (see parameters in figure).

[13] Preliminary results on elastic scattering were presented by one of the authors (G. A. S.) at the April, 1960 meeting of the American Physical Society, Washington, D. C. (Bull. Am. Phys. Soc. **5**, 282 (1960).

[14] A partial analysis of elastic scattering and single meson production may be found in *The Proceedings of the 1960 Annual International Conference on High-Energy Physics at Rochester* (Interscience Publishers, New York, 1960), p. 203.

[15] R. Serber, Phys. Rev. **72**, 1114 (1947).

[16] S. Fernbach, R. Serber, and T. B. Taylor, Phys. Rev. **75**, 1352 (1949).

mb. It was clear from Fig. 3 that for all except large scattering angles, a purely diffracting disk fit the data quite well. Also it was evident that some phase shift and/or tapering of the proton edge was required to fit the large-angle scattering. The radius found in this experiment for the purely absorbing disk is in agreement with radii found at 2.24 and 4.40 Bev by Cork *et al.*[2] General agreement with their results is also obtained in models B and C. The extrapolated value of the forward scattering amplitude in this experiment is consistent with a negligible amount of real potential scattering using the optical theorem. However the results of Preston *et al.*[5] indicate a somewhat larger forward scattering amplitude.

In order to look for possible polarization effects in the proton-carbon scattering, a right-left asymmetry parameter, $\epsilon=(R-L)/(R+L)$, was calculated for all proton-proton scatters in the chamber. The first scatter off carbon was to the right. The net asymmetry observed at all laboratory scattering angles was $-3.3\pm3.1\%$, consistent with the assumption that small if not negligible polarization effects were observed in the experiment. Also, no appreciable asymmetries as a function of laboratory scattering angle in the second scattering were observed.

VI. INELASTIC INTERACTIONS

A total of 1655 two-prong inelastic events were analyzed in this experiment.[14] Based on events in a selected fiducial volume in the chamber, the inelastic two-prong cross sections were determined and are given in Table I. Also included are the $pn\pi^+/pp\pi^0$ branching ratio, and the ratio of two-prong multiple meson production to single meson production (excluding $d\pi^+$).

It is of interest to investigate the $pn\pi^+/pp\pi^0$ branching ratio in terms of various models developed to interpret meson production in nucleon-nucleon collisions. Fermi[17] has developed a statistical model in which it is assumed that the nucleon-nucleon collision releases the total center-of-mass energy E into a small volume $\Omega=2M\Omega_0/E$, where Ω_0 is a spherical volume of one pion Compton wavelength radius. This energy is distributed very rapidly among the various degrees of freedom available in the volume according to statistical laws. In the absence of any final state interaction between the nucleons and pions, the ratios of these different single-pion charge states is just three to one. Peaslee[18,19] has proposed that since the pion and nucleon have shown strong resonance effects (particularly at 154-Mev π-N Q-value for the $T=\frac{3}{2}$, $J=\frac{3}{2}$ state), the production might proceed through an intermediate isobaric state which subsequently decays. In such a model, $pn\pi^+/pp\pi^0$ is five. Cerulus and Hagedorn[20] have recently made a calculation at 2.75 Bev in which both final states involving non-interacting particles, and final states in which a $T=\frac{3}{2}$ isobar is produced, are formed according to statistical laws. That is, the probability for the formation of N nucleons, N^* isobars, and ν pions, is given by $\Omega^{N+N^*+\nu-1}f_{T,S}\rho(E)$, where $f_{T,S}$ is a statistical factor taking into account the number of real-spin and isotopic-spin states available and the indistinguishability of like particles, and $\rho(E)$ is the number of nucleon, isobar, and pion final states per unit energy for a total c.m. energy of E. This model predicts that the ratio $pn\pi^+/pp\pi^0$ is 3.41 and that the ratio of two-prong multiple-meson production to single-meson production is 1.30.

TABLE I. Inelastic two-prong cross sections.

$pn\pi^+$	11.44±0.65 mb
$pp\pi^0$	2.90±0.31 mb
$d\pi^+$	0.11±0.06 mb
multiple meson	7.37±0.51 mb
$pn\pi^+/pp\pi^0$	3.94±0.48
multiple meson/$(pn\pi^++pp\pi^0)$	0.514±0.043

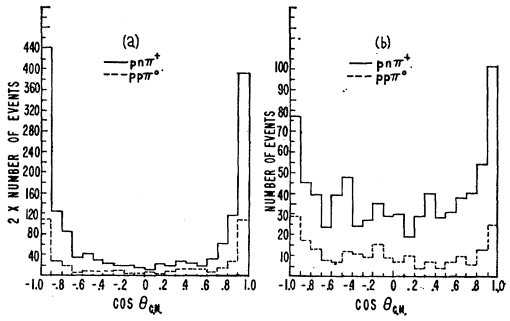

FIG. 4. (a) Nucleon c.m. angular distributions. (b) Pion c.m. angular distributions.

The experimental nucleon and pion c.m. angular distributions are shown in Fig. 4. Since in the proton-proton c.m. system the "forward" and "backward" directions are indistinguishable, the distributions should be symmetric about 90°. The distributions showed no evidence for deviation from this symmetry. As can be seen in Fig. 4, the nucleons showed a very strong tendency to scatter along the direction of motion of the p-p center of mass. This suggested that perhaps the incident protons underwent a peripheral collision with high relative-angular momentum. In order to estimate the magnitude of the angular momentum involved in these collisions, the proton and neutron distributions for $pn\pi^+$ were folded about 90°, and an even power of $\cos\theta_{\text{c.m.}}$ was fit to the interval $0.85<\cos\theta_{\text{c.m.}}<1.0$ for the protons, and $0.90<\cos\theta_{\text{c.m.}}<1.0$ for the neutrons. The best-fit powers were found to be ten and sixteen, respectively. This implied that small-angle proton production was in states of $l\gtrsim5$, whereas small-angle

[17] E. Fermi, Progr. Theoret. Phys. (Kyoto) **5**, 570 (1950).

[18] D. C. Peaslee, Phys. Rev. **94**, 1085 (1954).

[19] D. C. Peaslee, Phys. Rev. **95**, 1580 (1954).

[20] F. Cerulus and R. Hagedorn, CERN Report 59-3, 1959 (unpublished).

neutron production was in states of $l \gtrsim 8$. In terms of a semiclassical model, the scattering radius for a proton with c.m. momentum 1156 Mev/c and angular momentum $l\hbar$ is given by $R=l\hbar/p=1.70l\times10^{-14}$ cm, which gives $R=1.36\times10^{-13}$ cm for $l=8$, and $R=0.85\times10^{-13}$ cm for $l=5$. These results are consistent with the assumption that single meson production results from collisions of protons separated in the c.m. system by a radius of interaction of about 0.6-1.0 pion Compton wavelengths.

The experimentally observed Q-value distributions for $pn\pi^+$ and $pp\pi^0$ are shown in Figs. 5 and 6(a). The Q value is defined as the total kinetic energy of the pion and nucleon in their own center-of-mass system. From many earlier experiments[21] it was well known that the π^- and π^+ resonate with the nucleon in a $T=\frac{3}{2}$ state, with total center-of-mass kinetic energy peaked at about 154±50 Mev. The π^+-p total cross section has been normalized to the number of events in the interval 150–175 Mev, and is shown in Fig. 5(a). In addition, the prediction of the Fermi statistical model without isobars (phase space), normalized to the area in the histogram, is shown.[22] In the area of 150 Mev the π^+-p Q-value distribution showed excellent agreement with the π^+-p total cross section. It was noted that the prediction of the Fermi statistical model without isobars was completely inconsistent with the observed distribution. Lastly, possibly because of the phase-space limitation, at higher Q values no additional $T=\frac{3}{2}$ resonances were observed (it is believed that the π^+-p total cross section peaks at $Q\sim820$ Mev in a $T=\frac{3}{2}$ state[23]).

In an attempt to see a $T=\frac{3}{2}$-peak in the π^+-n case, all "resonant-π^+p" events were subtracted from the total Q-value distribution of Fig. 5(b). However, assuming that a $T=\frac{3}{2}$ isobar is formed in every collision as in the Peaslee model, the intensity for the process

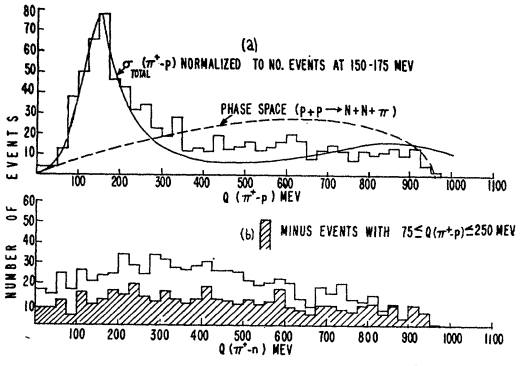

FIG. 5. (a) π^+-p Q-value distribution for $pn\pi^+$ with the known π^+-p total cross section normalized to the number of events at 150–175 Mev (solid curve) and three-body phase space (dashed curve). (b) π^+-n Q-value distribution for $pn\pi^+$ for (1) all events and (2) events with $Q(\pi^+$-$p)$ less than 75 Mev and greater than 250 Mev.

[21] S. J. Lindenbaum, Ann. Rev. Nuc. Sci. **7** (1957).
[22] M. M. Block, Phys. Rev. **101**, 796 (1956).

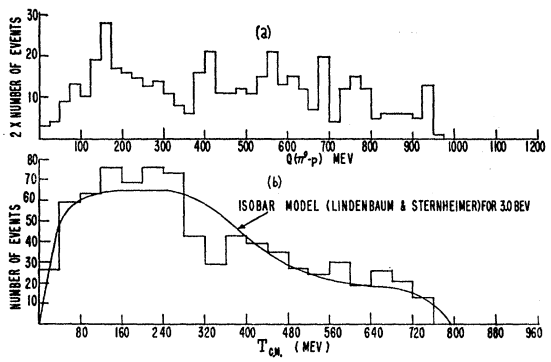

FIG. 6. (a) π^0-p Q-value distribution for $pp\pi^0$. (b) Pion c.m. kinetic energy distribution with the prediction of the isobar model of Lindenbaum and Sternheimer at 3.0 Bev normalized to the area in the histogram for $pn\pi^+$.

$p+p\rightarrow N+N^*$, $N^*\rightarrow n+\pi^+$ should be only 1/9 that for the process $p+p\rightarrow N+N^*$, $N^*\rightarrow p+\pi^+$. This factor greatly reduced any $T=\frac{3}{2}$ effect in the π^+-n relative to the background. The π^0-p distribution of Fig. 6(a) showed the $T=\frac{3}{2}$ peak. Since the intensity for the process $p+p\rightarrow N+N^*$, $N^*\rightarrow p+\pi^0$ in the $T=\frac{3}{2}$ state is 2/9 that for $p+p\rightarrow N+N^*$, $N^*\rightarrow p+\pi^+$, the peak had twice the magnitude of the π^+-n peak but much less background. There is now evidence[23] that a $T=\frac{1}{2}$ resonance exists at $Q\sim435\pm15$ Mev and $Q\sim609\pm15$ Mev. The experimental π^0-p and "nonresonant-π^+p" π^+-n Q-value distributions showed some evidence for the presence of these states.

The data presented so far have provided considerable evidence to support the assumption that a $T=\frac{3}{2}$ π-N isobar plays an important role in inelastic p-p collisions at 2.85 Bev. Several workers have made theoretical predictions based on some form or another of an isobar model.[24,25] The work of Lindenbaum and Sternheimer[24] shows excellent agreement with the data. It is assumed by Lindenbaum and Sternheimer that in every collision a $T=\frac{3}{2}$ isobar is formed and that the probability for forming an isobar of a given mass is directly related to the known π^+-p cross section at that mass and a two-body (nucleon, isobar) phase-space factor evaluated for that mass. Other than for initial energy and momentum transfer, the isobar does not interact with the recoil nucleon. Assuming that the isobar decays isotropically in its own rest frame, the nucleon (both recoil and decay) and pion kinetic energy spectra are numerically evaluated by integration over all possible mass values. The final nucleon spectra are then obtained by apportioning the correct amount of recoil and decay intensities according to charge independence. The experimental c.m. kinetic energy distributions are given in Figs. 6(b) and 7. Theoretical 3.0-Bev nucleon spectra

[23] T. J. Devlin, B. C. Barish, W. N. Hess, V. Perez-Mendez, and J. Solomon, Phys. Rev. Letters **4**, 242 (1960).
[24] S. J. Lindenbaum and R. M. Sternheimer, Phys. Rev. **105**, 1874 (1957).
[25] Saul Barshay, Phys. Rev. **106**, 572 (1957).

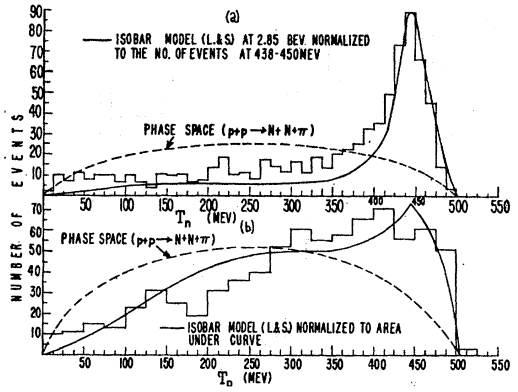

FIG. 7. (a) Neutron c.m. kinetic energy distribution for $pn\pi^+$, with the prediction of the isobar model (L. & S.) at 3.0 Bev rescaled to an upper limit of 503 Mev for 2.85-Bev p-p collisions. (b) Proton c.m. kinetic energy distribution for $pn\pi^+$, with the prediction of the isobar model (L. & S.) at 3.0 Bev rescaled to an upper limit of 503 Mev for 2.85-Bev p-p collisions.

have been rescaled slightly to give the correct upper-limit kinetic energy of 503 Mev for the nucleons at 2.85 Bev. The theoretical pion spectrum is for 3.0 Bev.[26] All spectra showed good agreement with the theory.

It is well known that the $T=\frac{3}{2}$-isobaric state has total angular momentum $J=\frac{3}{2}$. If the isobar were produced polarized or aligned, then the state of this polarization or alignment would be normal to the plane of production.[27] For instance, an isobar with $M_J=\pm\frac{3}{2}$ decaying free of interaction with the recoil nucleon and conserving parity in the decay would have a decay distribution in its own rest frame of the form $\sin^2\gamma$, where the axis of quantization has been selected normal to the plane of production in the laboratory and the angle γ is measured with respect to the direction $\mathbf{k}_{\text{isobar}}\times\mathbf{k}_{\text{beam}}$, where $\mathbf{k}_{\text{isobar}}$ and $\mathbf{k}_{\text{beam}}$ are unit vectors along the direction of the isobar and beam track in the laboratory respectively. The experimental distribution is shown in Fig. 8(a). Only events with $80<Q(\pi^+p)<220$ Mev were selected to reduce the non-isobaric background to a minimum. The distribution was consistent with isotropy and showed no effect of polarization or alignment in $M_J=\pm\frac{3}{2}$ or $\pm\frac{1}{2}$ states (population of $J=\frac{3}{2}$, $M_J\pm\frac{1}{2}$ states gives a $1+3\cos^2\gamma$ distribution).

In view of the observed distributions, it was considered possible that single-pion exchange processes were important, if not dominant, in the collisions. In order to investigate this feature in single-pion production, the diagram of Fig. 9 was considered for $pn\pi^+$ events. Since the authors had successfully discriminated the cross section at the scattering vertex in the $T=\frac{3}{2}$ resonance, as compared to higher energy nonresonant scattering by a Chew-Low extrapolation,[28] it was hoped that one could also measure the known elastic π^+-p scattering angular distribution in the resonance. It is well known[29] that at the $T=\frac{3}{2}$, $J=\frac{3}{2}$ resonance the π^+-p elastic scattering exhibits a $1+3\cos^2\theta_\pi^*$ distribution, where θ_π^* is the angle of the scattered pion measured in the π^+-p c.m. system with respect to the direction of the incident pion. Below and above the resonance the distribution becomes asymmetric, peaked backward and forward, respectively. *Assuming* that energy was conserved in the virtual process (the pion direction was determined since momentum is conserved in the virtual process), the angle of scattering of the pion was calculated for all $pn\pi^+$ events with $80<Q(\pi^+p)<220$ Mev. Since the laboratory system and the rest system of the incident proton are completely equivalent in the p-p collision, the event was treated in that system in which the neutron momentum was higher. It was assumed here that it was more likely for a projectile proton of high momentum to emit a high-momentum neutron than for a stationary proton to do so. It should be pointed out that, in terms of the isobar model, θ_π^* is just the isobar decay angle in its rest frame measured with respect to its direction in that system in which the neutron has the higher momentum. The "scattering" distribution is shown in Fig. 8(b). The distribution was consistent with isotropy. It was not certain to what extent nonconservation of energy by the pion at the emission and scattering vertices affected the results.

VII. CONCLUSIONS

From a study of 2693 two-prong proton-proton interactions at a laboratory energy of 2.85 Bev, the following results have been obtained:

1. The elastic scattering cross section is 15.32 ± 0.76 mb. The differential cross-section peaks strongly to 40 ± 2 mb/steradian in the c.m. system at 0°. In terms of an optical model, the scattering is explained almost

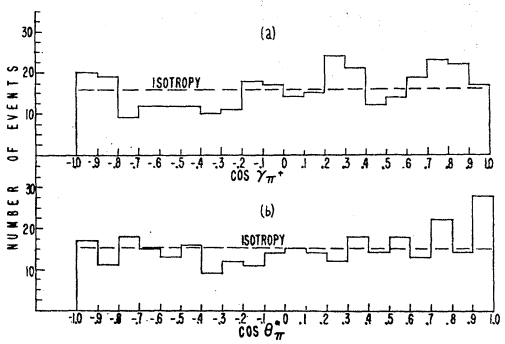

FIG. 8 (a) Isobar [$80<Q(\pi^+$-$p)<220$ Mev] decay angular-distribution in the isobar rest frame relative to the normal to the neutron, isobar production plane. (b) Isobar [$80<Q(\pi^+$-$p)<220$ Mev] decay angular distribution in the isobar rest frame relative to its direction in the laboratory.

[26] The authors wish to thank Dr. R. M. Sternheimer of Brookhaven National Laboratory for sending them unpublished 3.0-Bev isobar calculations.

[27] L. Wolfenstein, Phys. Rev. **75**, 1664 (1949).

[28] G. A. Smith, H. Courant, E. C. Fowler, H. Kraybill, J. Sandweiss, and H. Taft, Phys. Rev. Letters **5**, 571 (1960).

[29] W. O. Lock, *High-Energy Nuclear Physics* (John Wiley & Sons, Inc., New York ,1960), Chap. IV.

entirely by a pure diffraction type scattering up to about 35° in the c.m. system. At angles above 35° some phase shift and/or tapering to the edges of the proton is required to fit the data. No polarization effects are observed in the elastic scatter of the protons from carbon using hydrogen as an analyzer of polarized protons.

2. The $pn\pi^+$ cross section is 11.44±0.65 mb. The nucleons are strongly peaked at 0° and 180° in the c.m. system, suggesting the presence of dominant high-angular-momentum states. The π^+-p Q-value distribution provided strong evidence that a $T=\frac{3}{2}$ isobar is formed in at least 50% of the collisions. Calculations by Lindenbaum and Sternheimer on an isobar model, which allows for $T=\frac{3}{2}$ isobar formation based on the known π^+-p cross section and a two-body (isobar, nucleon) phase-space factor, assuming that the isobar decays isotropically in its center-of-mass system, show good to excellent agreement with the observed neutron, proton, and pion energy spectra. No evidence for scattering in a pure $J=\frac{3}{2}$ state by a virtual π^+, emitted from the projectile proton, on the target proton is observed if one assumes that energy is conserved at the emission and scattering vertices. Assuming that the total angular momentum of the isobar is $J=\frac{3}{2}$, there is no evidence that the isobar is produced polarized or aligned in states with $M_J=\pm\frac{3}{2}$ or $\pm\frac{1}{2}$. Very weak evidence for the known $T=\frac{1}{2}$ resonances at $Q=435$, 609 Mev is observed. The energy spectra are clearly inconsistent with the prediction of a statistical model without isobars.

3. The $pp\pi^0$ cross section is 2.90±0.31 mb. As in the $pn\pi^+$ case the nucleons show a strong peaking at 0° and 180° in the c.m. system. The c.m. proton and pion energy spectra show general agreement with the isobar model of Lindenbaum and Sternheimer. Since the spectator and decay protons are indistinguishable, analysis in terms of the isobar model is not as clear-cut as in the $pn\pi^+$ case.

4. The $d\pi^+$ cross section is 0.11±0.06 mb. The cross section for multiple meson production in two-prong interactions is 7.37±0.51 mb.

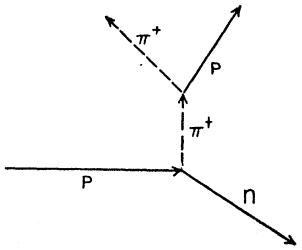

Fig. 9. Diagram corresponding to the emission of a virtual pion by the projectile proton in the laboratory and the subsequent elastic scattering of the pion off the target proton.

5. The $pn\pi^+/pp\pi^0$ branching ratio is 3.94±0.48. This number is clearly inconsistent with the prediction of three from a statistical model without isobars and with the Peaslee model prediction of five with $T=\frac{3}{2}$ isobars being formed in every collision. The inclusion of isobar formation in the statistical model in proportion to the available isobar-nucleon phase space, geometrical, and statistical factors of the model as given by Cerulus and Hagedorn, predicts a value of 3.41. The ratio of multiple meson production in two-prong events to single meson production is 0.514±0.043. This is not in agreement with the prediction of 1.30 as given by Cerulus and Hagedorn.

ACKNOWLEDGMENTS

To Dr. Ralph Shutt and members of the Brookhaven Bubble Chamber Group the authors express their gratitude for the use and operation of the bubble chamber and for generous sharing of film during the course of analysis of the pictures. The authors also thank Dr. George Collins and members of the Brookhaven Cosmotron Department for their effective operation of the Cosmotron during the experiment. The use of computing facilities at the Yale University Computing Center and the A.E.C. Computing and Applied Mathematics Center, Institute of Mathematical Sciences, New York University, is gratefully acknowledged.